

Correlation between Coil Configurations and Discharge Characteristics of a Magnetized Inductively Coupled Plasma

Hee-Woon Cheong*

Graduate School of Management of Technology, Hoseo University, Asan 31499, Korea

(Received 4 March 2016, Received in final form 3 May 2016, Accepted 25 May 2016)

Correlation between coil configurations and the discharge characteristics such as plasma density and the electron temperature in a newly designed magnetized inductively coupled plasma (M-ICP) etcher were investigated. Radial and axial magnetic flux density distributions as well as the magnetic flux density on the center of the substrate holder were controllable by placing multiple circular coils around the etcher. The plasma density increased up to 60.7 % by arranging coils (or optimizing magnetic flux density distributions inside the etcher) properly although the magnetic flux density on the center of the substrate holder was fixed at 7 Gauss.

Keywords : M-ICP, Magnetic flux density, Plasma density

1. Introduction

The increase in density of semiconductor device integration and the design rule shrinkage make the requirements of dry etchers more stringent. In this regard, a number of high performance plasma etchers such as an inductively coupled plasma (ICP) etcher [1, 2], an electron cyclotron resonance (ECR) etcher [3-5] and so on [6] have been developed or are currently under development. Especially, it had been reported that a magnetized inductively coupled plasma (M-ICP) etcher generates high-density plasma and guarantees a high etch rate of etching materials by applying a weak and controllable magnetic field to the conventional ICP etcher [7].

In this paper, two-dimensional magnetic flux density distributions inside the M-ICP etcher according to coil configurations were investigated when the magnetic flux density on the center of the substrate holder was fixed at 7 Gauss. Plasma density, electron temperature and plasma density non-uniformity characteristics of the M-ICP etcher according to coil configurations were also studied.

2. Experimental setup

Figure 1 shows the schematic of the M-ICP etcher. The

etcher is powered by two rf generators. One is the source power generator which supplies 27.12 MHz rf power to a two-turn planar antenna and the other is the bias power generator which supplies 2 MHz and/or 13.56 MHz rf power to the substrate holder whose diameter is 300 mm. A chiller using ethylene glycol as a refrigerant maintains the substrate holder temperature at 15 °C during the

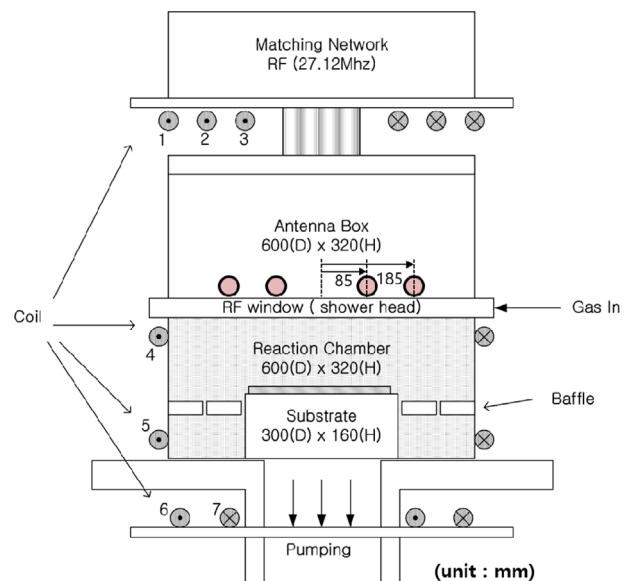


Fig. 1. (Color online) Schematic of M-ICP etcher with seven circular coils (coil 1, 2, 3, 6, 7 : 1400 turns, coil 4, 5 : 1000 turns).

Table 1. Electric currents applied to coils 1~7.

	Coil 1	Coil 2	Coil 3	Coil 4	Coil 5	Coil 6	Coil 7
Case 1	N/A	N/A	N/A	250 mA	250 mA	N/A	N/A
Case 2	140 mA	140 mA	140 mA	140 mA	140 mA	140 mA	140 mA
Case 3	N/A	N/A	500 mA	500 mA	500 mA	-750 mA	N/A
Case 4	N/A	N/A	500 mA	500 mA	500 mA	N/A	-750 mA
Case 5	N/A	N/A	750 mA	750 mA	750 mA	-750 mA	-750 mA
Case 6	350 mA	350 mA	350 mA	350 mA	350 mA	-750 mA	350 mA
Case 7	330 mA	330 mA	330 mA	330 mA	330 mA	330 mA	-750 mA

experiments. The etcher is pumped by a 3500 l/s turbo-molecular pump and the base pressure for the experiment was 0.004 Pa. Discharge gas, whose flow rate is regulated by the mass flow controller (MFC), flows into the etcher through a gas inlet and the resultant neutral gas pressure is measured by the hot-filament ionization gauge and baratron gauge (Granville-Phillips® 392 Micro-Ion® Plus). A 20 mm-thick rf window made of alumina-based ceramic is employed to allow the power transfer from antenna to plasma.

Meanwhile, the magnetic fields are generated using seven circular coils. Firstly, three coaxial coils (1~3) are placed on top of antenna box. The number of turns of each copper coil is 1400. Secondly, two coaxial coils (6, 7) are located at the bottom of the frame shown in the figure and the number of turns of each coil is also 1400. Lastly, two coils (4, 5) are located at upper and lower sides of the chamber. The number of turns of each coil is 1000. With these coils, seven different cases of coil configurations were set up as shown in Table 1 to study the correlation between the magnetic flux density distributions inside the etcher and the discharge characteristics of M-ICP. The number of coils that electric current is applied to and the electric current value supplied to coils vary in different cases. The magnetic flux density on the center of the substrate holder in all cases was fixed at 7 Gauss.

The two-dimensional magnetic flux density distributions inside the etcher were simulated with the finite element method magnetic (FEMM) field calculation software when the magnetic flux density on the center of the substrate holder was fixed at 7 Gauss. Meanwhile, the radial plasma density distributions inside the M-ICP etcher were measured using a dual Langmuir probe (DLP) [8]. The vertical height of DLP from the substrate holder was 10 mm. The radial distance of the probe tips from the center of the substrate holder was varied from 0 to 160 mm at 20 mm intervals. The plasma density non-uniformity was also calculated using:

$$\text{Non-uniformity (\%)} = \frac{(\text{maximum of plasma density} - \text{minimum of plasma density})/2}{\text{average of plasma density}} \quad (1)$$

3. Results and Discussion

Figure 2 shows the radial and axial magnetic flux density distributions from the center of the substrate holder according to coil configurations. The magnetic flux density in M-ICP case 1 and that in M-ICP case 2 decrease both radially and axially, whereas those in M-ICP case 3~7 increase both radially and axially due to coil 6 and/or coil 7 whose current flow is in the reverse direction. The radial magnetic flux density distribution inside the etcher should be considered carefully because it deeply affects the plasma density non-uniformity [9], as will be shown later. Meanwhile, the axial magnetic flux density distribution determines a right-hand circularly polarized wave (R-wave) propagation [10].

Figure 3 shows two-dimensional magnetic flux density distributions inside the M-ICP etcher. The magnetic flux density vectors from coil 6 and/or coil 7 in M-ICP case 3~7 counteract the effect of the vectors from coils 1~5, whose current flow are in the forward direction, around the center of the substrate holder, which may lead to the radial and axial increase in the magnetic flux density.

Figure 4 and Fig. 5 show plasma density and electron temperature inside the etcher when the neutral gas pressure was 0.67 Pa and 1.33 Pa, respectively. In this experiment, Ar flow rate was fixed at 60 sccm and the source power was fixed at 1000 W. The substrate holder was grounded. As expected from previous studies [7], M-ICP case 1~7 show higher plasma density than ICP does, whereas the electron temperature in M-ICP is almost similar to that in ICP. It is notable that plasma density varies in different M-ICP cases although the magnetic flux density on the center of the substrate holder was

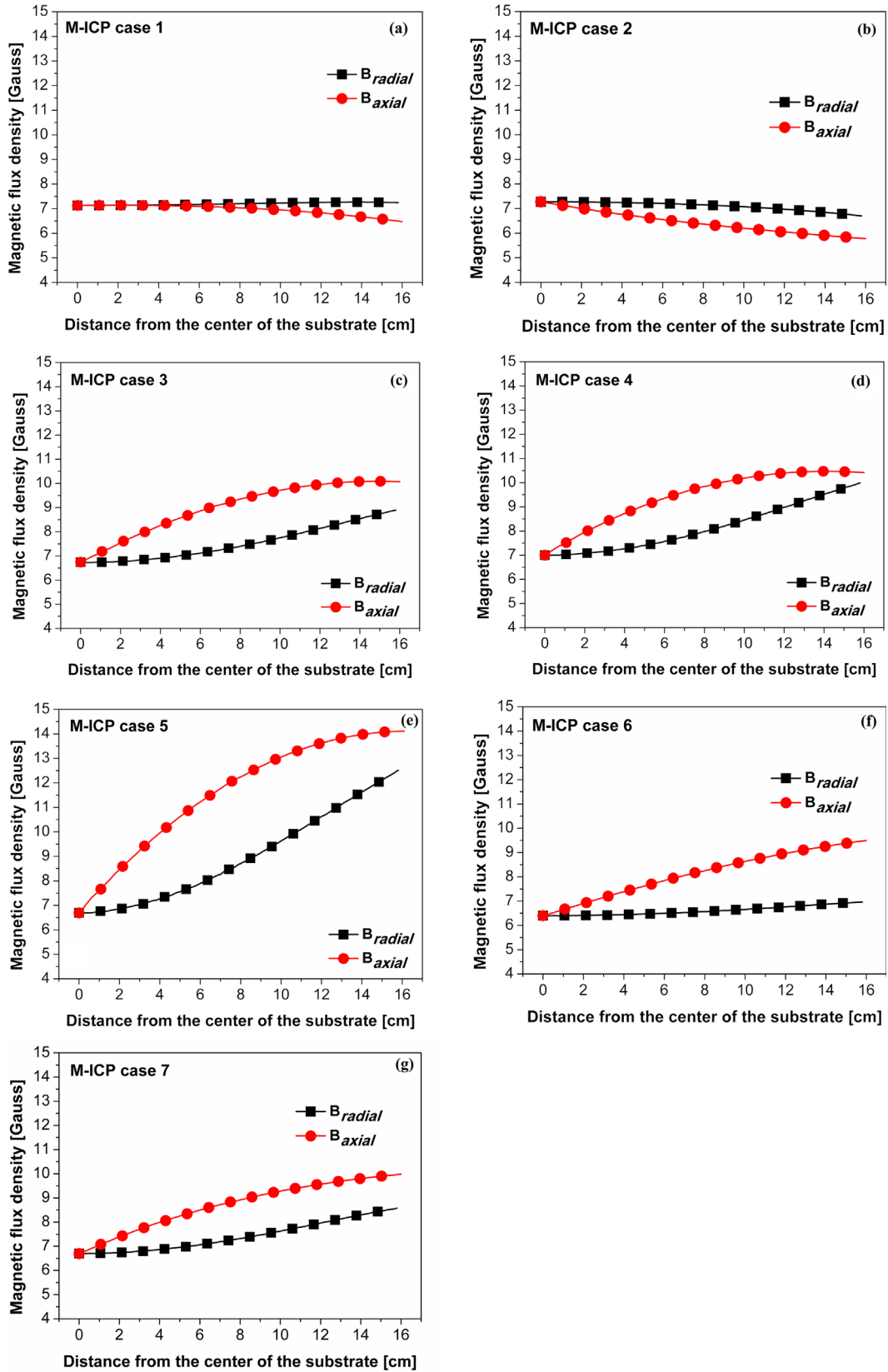


Fig. 2. (Color online) Radial and axial magnetic flux density distributions of (a) M-ICP case 1 (b) M-ICP case 2 (c) M-ICP case 3 (d) M-ICP case 4 (e) M-ICP case 5 (f) M-ICP case 6 and (g) M-ICP case 7 when the magnetic flux density on the center of the substrate holder is fixed at 7 Gauss.

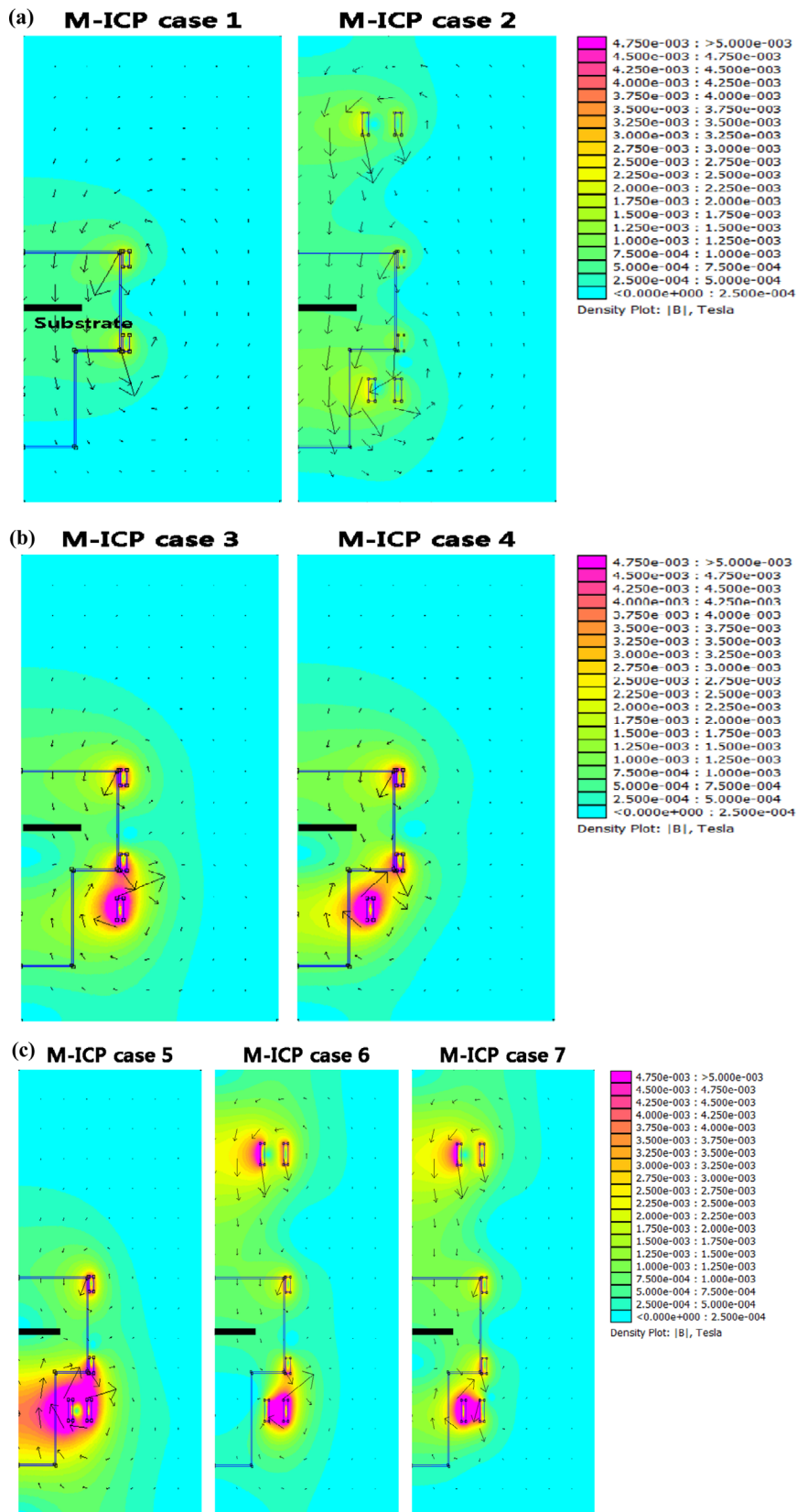


Fig. 3. (Color online) Two-dimensional magnetic flux density distributions of (a) M-ICP case 1 and case 2 (b) M-ICP case 3 and case 4 and (c) M-ICP case 5, case 6 and case 7 when the magnetic flux density on the center of the substrate holder is fixed at 7 Gauss.

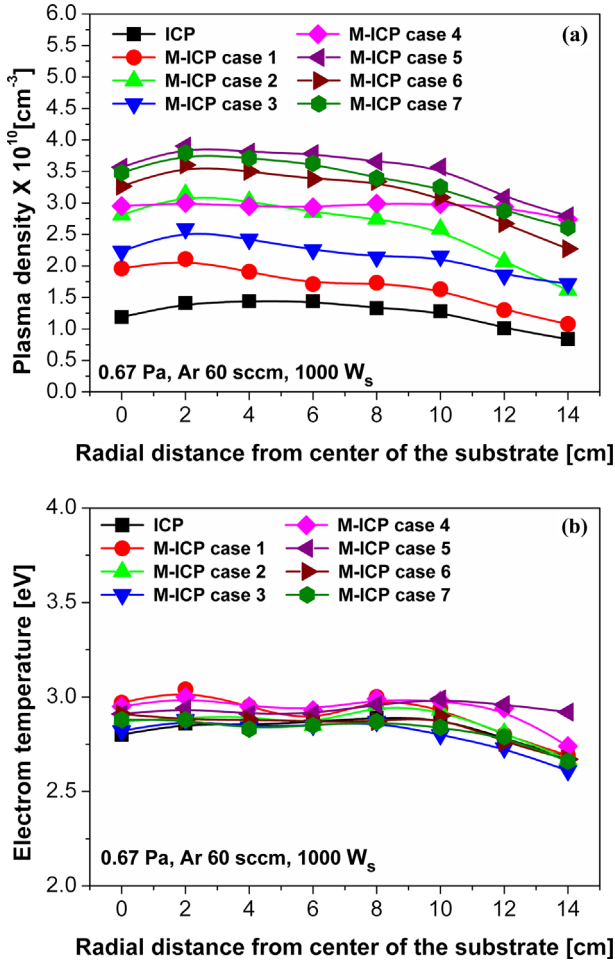


Fig. 4. (Color online) (a) Plasma density and (b) electron temperature according to coil configurations when the neutral gas pressure is 0.67 Pa.

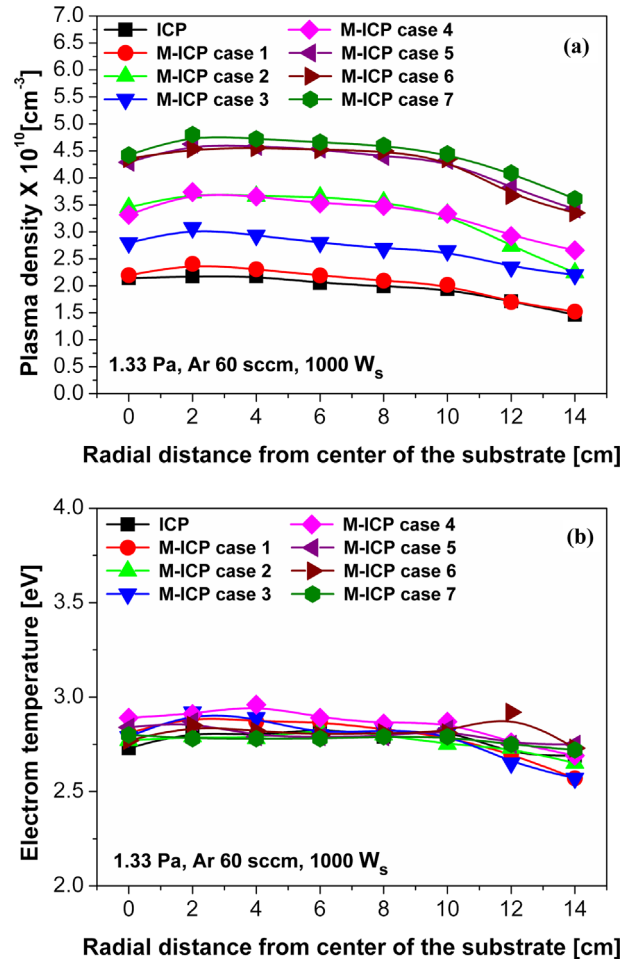


Fig. 5. (Color online) (a) Plasma density and (b) electron temperature according to coil configurations when the neutral gas pressure is 1.33 Pa.

fixed at 7 Gauss.

It can be confirmed more clearly in Fig. 6, which depicts plasma density and the electron temperature on the center of the substrate holder according to coil configurations and the neutral gas pressure, that the plasma density increases up to 60.7 % (M-ICP case 3 vs M-ICP case 7 @ 1.33 Pa) although the magnetic flux density on the center of the substrate holder is the same. Overall, M-ICP case 5~7 show higher plasma density than M-ICP 1~4 do.

The difference in plasma density among M-ICP case 1~7 can be explained by plasma confinement in a magnetic mirror field and mirror ratio (R_m) can be defined as follows [11] :

$$R_m = B_m/B_0 \tag{2}$$

where B_0 is the magnetic flux density on the substrate and B_m is the magnetic flux density around the rf window in

our experiment. The larger the value of R_m is, the stronger the plasma confinement would become.

Figure 7 shows the axial magnetic flux density distributions plotted from the substrate holder to coils 1~3 according to coil configurations. M-ICP case 5 shows the largest R_m among all cases, which may lead to higher plasma density compared to M-ICP case 1~4. R_m of M-ICP case 6 or that of case 7 is lower than that of M-ICP case 5. However, the plasma density of M-ICP case 6 or that of case 7 is higher than those of M-ICP 1~4 and is similar to that of M-ICP case 5 due to the continuous increase in the axial magnetic flux density, which is necessary and sufficient condition for magnetic mirroring or plasma confinement [11].

On the other hand, the plasma density of M-ICP case 3 or that of case 4 is lower than those of M-ICP 5~7 because the axial magnetic flux density starts to decrease from beneath the rf window and the plasma confinement

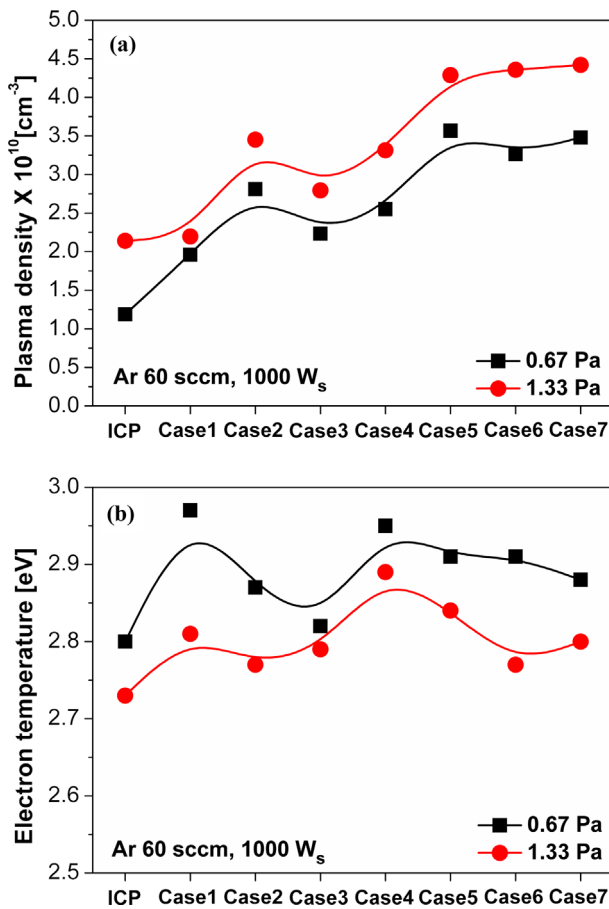


Fig. 6. (Color online) (a) Plasma density and (b) electron temperature on the center of the substrate holder according to coil configurations and the neutral gas pressure.

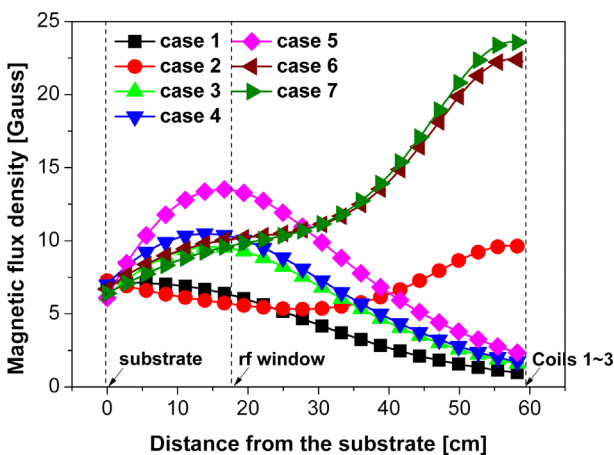


Fig. 7. (Color online) Axial magnetic flux density distributions according to coil configurations.

is weakened. Needless to say, M-ICP case 1 or case 2 shows relatively lower plasma density than another cases do because the axial magnetic flux density shows continuous decrease from the substrate holder to the rf

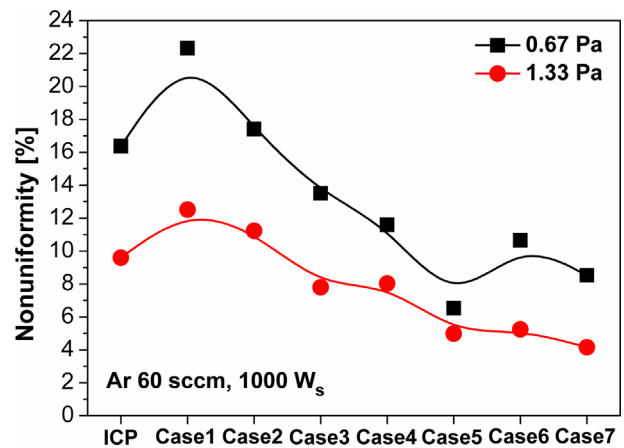


Fig. 8. (Color online) Plasma density non-uniformity according to coil configurations and the neutral gas pressure.

window.

Figure 8 shows plasma density non-uniformity according to coil configurations and the neutral gas pressure. M-ICP case 3~7 show lower non-uniformity (or higher uniformity) than M-ICP case 1 or case 2 does because the radial decrease in the magnetic flux density in M-ICP case 1 or that in case 2 may cause the flute instability [9].

Overall, M-ICP case 5~7 show higher plasma density and plasma density non-uniformity than M-ICP case 1~4 do. However, M-ICP case 7 is thought to be the best configuration since the power consumption is the lowest among three cases based on Table 1.

4. Conclusion

Magnetic flux density distributions inside the newly designed M-ICP etcher were investigated. It was confirmed that the magnetic flux density increased radially from the center of the substrate holder because the coils whose current flow are in the reverse direction counteract the effect of the magnetic flux density vectors generated from coils, whose current flow are in the forward direction, around the center of the substrate holder.

Meanwhile, the plasma density varies in different M-ICP cases although the magnetic flux density on the center of the substrate holder was fixed at 7 Gauss because the plasma density is not only determined by the magnetic flux density but also R_m and the axial magnetic flux density distribution from the substrate holder to the rf window. As a result, the plasma density could be increased up to 60.7 % by optimizing the magnetic flux density distribution inside the etcher properly.

More importantly, the best coil configuration for M-ICP can be determined based on the plasma density, plasma

density non-uniformity and the amount of electrical power consumed by coils.

Acknowledgements

This work has been supported by Prof. Ki-Woong Whang of the Inter-university Semiconductor Research Center (ISRC) in Seoul National University, Seoul, Korea and the Graduate school of Technology Management in Hoseo University, Asan, Korea.

References

- [1] S. Imai, *J. Vac. Sci. Technol. B* **26**, 2008 (2008).
- [2] A. C. Westerheim, A. H. Labun, J. H. Dubash, J. C. Arnold, and H. H. Sawin, *J. Vac. Sci. Technol. A* **13**, 853 (1995).
- [3] H. H. Doh, C. K. Yeon, and K. W. Whang, *J. Vac. Sci. Technol. A* **15**, 664 (1997).
- [4] K. Nojiri and E. Iguchi, *J. Vac. Sci. Technol. B* **13**, 1451 (1995).
- [5] T. Maruyama, T. Narukage, R. Onuki, and N. Fujiwara, *J. Vac. Sci. Technol. B* **28**, 854 (2010).
- [6] S. Hosomi and N. Omori, *J. Vac. Sci. Technol. A* **15**, 585 (1997).
- [7] H. J. Lee, J. H. Kim, K. W. Whang, and J. H. Joo, *J. Vac. Sci. Technol. A* **14**, 1007 (1996).
- [8] Y. Sung, H. B. Lim, and R. S. Houk, *J. Anal. At. Spectrom* **17**, 565 (2002).
- [9] W. H. Lee, H. W. Cheong, J. W. Kim, and K. W. Whang, *Plasma Sources Sci. Technol.* **24**, 065012 (2015).
- [10] H. W. Cheong, *J. Magn.* **20**, 360 (2015).
- [11] F. F. Chen, *Introduction to Plasma Physics and Controlled Fusion*, Plenum Press, New York and London (1984).